Journal of Maritime Research, Vol. VII. No. 2, pp. 73–88, 2010
Copyright © 2010. SEECMAR

ISSN: 1697-4840

DESIGN ASPECTS AND TWO-DIMENSIONAL CFD SIMULATION OF A MARINE PROPULSOR BASED ON A BIOLOGICALLY-INSPIRED UNDULATING MOVEMENT

M.I. Lamas[1,2], J.D. Rodríguez[1], C. G. Rodríguez[1] and P. B. González[1]

Received 06 May 2010; in revised form 14 May 2010; accepted 30 July 2010

Abstract

Nowadays, it is well known that aquatic animals have higher locomotion performance than man-made marine vehicles. There are a lot of researchers who have built different kinds of machines replicating the movement of animals. The principal problem is that it is very important to fully understand the hydrodynamics of biological swimming to design an optimal mechanism. For this reason, the CFD (Computational Fluid Dynamics) has become a very powerful technique because it solves the governing equations of conservation of mass and momentum so as to obtain the fluid flow characteristics.

This paper presents the development of a marine propulsor based on an undulating fin which emulates fish movement. Furthermore, an extensively CFD investigation of the fluid flow around the propulsor is presented. As experimental tests were performed on a scaled model rather on a real ship, a non dimensional analysis was done. Particularly, the non-dimensional governing groups analyzed were the Reynolds, Froude and Strouhal numbers. The CFD results compared reasonably well with the experimental ones obtained on the lab prototype.

Keywords: CFD, biomimetic, undulating fin, marine propulsion.

INTRODUCTION

Throughout history, the implementation of rotating propulsion mechanisms has been highly used because they are relatively easy to design. On the contrary, undulat-

[1] Escola Universitaria Politécnica, Universidade da Coruña, Avda. 19 de Febrero s/n, 15405, Ferrol, Spain. Tlf.: 981337400. Fax.: 981337416. [2] E-mail: isabellamas@udc.es.

ing mechanisms, which are very common in nature, have been poorly considered. Nowadays, engineering of marine vehicles and machines is changing and new propulsion methods are being studied, specially the biologically-inspired ones.

Biomimetic is an emerging field which employs the principles of living organisms to derive man-made mechanisms which are capable of emulating the efficient movement of animals. Given that most vertebrates are aquatic and have had hundreds of millions of years to adapt to that environment, it is reasonable to suppose that natural selection has optimally developed the kinematics of these animals. For this reason, it is expected that mechanisms which emulates fish movement are more efficient, versatile and maneuverable than classical rotating propellers. In the field of marine propulsion, there are a lot of researchers who applied the biomimetic to make ship propulsors, for example Barret *et al.* (1999) constructed a fish-like mechanism and studied it on a laboratory in order to compare the undulating fish movement with a rigid wall movement. They concluded that the power required to propel an actively swimming fish-like body is significantly smaller than the power needed to tow the body straight and rigid and they obtained drag reductions up to 70% for the undulating fish movement.

Zhang (2007) investigated the bionic neutral network control method for fish-robots.

Young-hua *et al.* (2007) designed an environment-friendly propulsion system mimicking undulating fins and developed a two-dimensional CFD method to study the unsteady flow around the fin. They focused its study on studying the amplitude configuration.

Bozkurtass *et al.* (2008) constructed a propulsor for an autonomous underwater vehicle based on the mechanical design and performance of a sunfish pectoral fin, and developed a three-dimensional numerical model.

Low (2008) constructed an underwater vehicle using a fin-like mechanism based on a series of connecting linkages which produce undulations similar to those produced by the fin rays.

The main problem is that there are many aspects about the undulating propulsion which are not well understood yet. An important technique which helps to answer a lot of decisive questions is the CFD (Computational Fluid Dynamics). The CFD is used to solve the governing equations so as to obtain the hydrodynamics of the fluid flow. In the field of numerical simulation, there are several researchers who applied the CFD to study the laminar and turbulent flow over a sinusoidally shaped solid surface. Bordner (1978) studied the laminar flow over a periodic wavy wall. Markatos (1978) used the k–ε model to study the heat, mass and momentum transfer at a wavy boundary. Caponi *et al.* (1982) developed a two-dimensional, laminar model. McLean (1983) developed a two-dimensional simple algebraic eddy-viscosity model to study the flow for small and larger amplitude waves. Patel *et al.* simulated the laminar (Patel *et al.*, 1991) and turbulent (Patel *et al.*, 1991) flow in a channel with a wavy wall.

This paper presents a design of a marine vehicle mimicking the undulating fin fish. In addition, a two-dimensional CFD model was developed to analyze the laminar flow over the propulsor. It is organized as follows. Firstly, details of the model and prescribed kinematics are presented. Secondly, the numerical method is briefly described. Thirdly, the hydrodynamic forces and other aspects are discussed and compared with experimental results. Finally, the conclusions of this work and an outline of areas for future research are presented.

NOMENCLATURE

L	[m]	Fin length	***Greek symbols***	
t	[s]	Time	τ [N/m^2]	Viscous stress tensor
F	[N]	Force	ρ [kg/m^3]	Density
C	[ ]	Force coefficient	ν [m^2/s]	Kinematic viscosity
A	[m^2]	Area		
n	[ ]	Unit normal vector	***Subscripts***	
V	[m/s]	Velocity	x	X direction
T	[1/s]	Period	F	Force
f	[Hz]	Frequency of oscillation	p	Pressure
P	[Pa]	Pressure	v	Viscosity
g	[m/s^2]	Gravity	∞	Free stream
Re	[ ]	Reynolds number		
Fr	[ ]	Froude number	***Superscripts***	
St	[ ]	Strouhal number	*	Non-dimensional

PROBLEM DEFINITION

Design and kinematics

"Innovacións Mariñas" Research Group (Coruña University-Spain) built a marine undulating propulsor. The prototype is shown in Fig. 1a and a detail of the undulating fin is shown in Fig. 1b. The fin was 0.52 m length and 0.1 m width.

(a) **(b)**

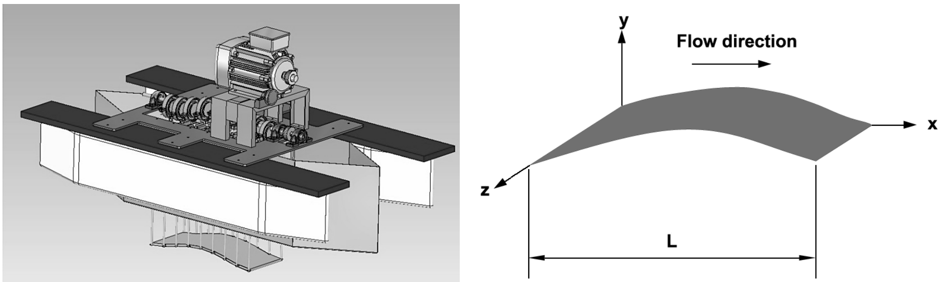

Figure 1. (a) Experimental prototype. (b) Detail of the fin.

The undulating motion is created by means of rods and connecting parts moved by an electric motor. Details of the mechanism were presented elsewhere (Rodríguez *et al.*, 2008).

An important advantage of this system is that it is reversible, *i.e.*, it has the same efficiency either operating forward or backward, which makes it ideal for vehicles that require high maneuverability.

CFD analysis

The flow around a travelling waving wavy wall is quite different from the flow around a rigid wall. As the fluid moves along the surface, the undulations from the anterior to the posterior fin produce thrust. Under the same conditions, a fish consumes much less energy to displace than a rigid body because the motion of the fish reduces turbulence effects. For this reason, the design of the wave is very important, and several CFD studies with different wave configurations were carried out before making the experimental prototype.

Governing equations

The flow motion is governed by the mass conservation equation and the Navier-Stokes equation, which for a laminar, Newtonian and constant properties fluid are given by Eqs. (1) and (2), respectively.

$$\nabla \cdot \vec{V} = 0 \tag{1}$$

$$\frac{\delta \vec{V}}{\delta t} + \nabla \cdot (\vec{V}\vec{V}) = -\frac{\nabla p}{\rho} + \nu \nabla^2 \vec{V} + \vec{g} \tag{2}$$

As mentioned above, tests were performed on a scaled model rather on a real ship, so a non-dimensional analysis was carried out. All the variables were converted to dimensionless quantities by introducing the reference parameters given in Table 1. The dimensionless variables, quoted with *, are also shown in this table.

Dimension	Reference parameter	Dimensionless parameter
Length	$L_{ref} = L$	$x^* = x / L_{ref}\,;\; y^* = y / L_{ref}$
Velocity	$V_{ref} = U_\infty$	$\vec{V}^* = \vec{V} / V_{ref}$
Pressure	$P_{ref} = \rho V_{ref}^2$	$P^* = P / P_{ref}$
Time	$t_{ref} = L_{ref} / V_{ref} = L / U_\infty$	$t^* = t / t_{ref}$
Gravity	$\vec{g}_{ref} = \vec{g}$	$\vec{g}_{ref} = \vec{g} / \vec{g}_{ref}$

Table 1. Reference and dimensionless parameters.

The resulting field equations in dimensionless form are shown as follows:

$$\nabla^* \cdot \vec{V}^* = 0 \tag{3}$$

$$\frac{\delta \vec{V}^*}{\delta t^*} + \nabla^* \cdot (\vec{V}^* \vec{V}^*) = -\nabla p^* + \frac{1}{\mathrm{Re}} \nabla^{*2} \vec{V}^* + \frac{1}{Fr^2} \vec{g}^* \tag{4}$$

where Re is the Reynolds number, defined by Eq. (5). It represents the relation between inertial and viscous effects.

$$\mathrm{Re} = \frac{U_\infty L}{\nu} \tag{5}$$

Fr is the Froude number, defined by Eq. (6). It represents the relation between inertial and gravity effects.

$$Fr = \frac{U_\infty}{\sqrt{Lg}} \tag{6}$$

In the equations above, U_∞ represents the free stream velocity.

NUMERICAL IMPLEMENTATION

Computational mesh

In order to implement the fin movement in the CFD code, it was necessary to use a dynamic mesh. The computational domain, as shown in Fig. 2a, was 3L height and 5L length (L is the fin length), and was discretized with 27000 nodes. The elements were triangular, and the size mesh was refined in the zone near the fin because this is the most critical area in terms of velocity and pressure gradients. A detail of the mesh in the zone closed to the fin is shown in Fig. 2b.

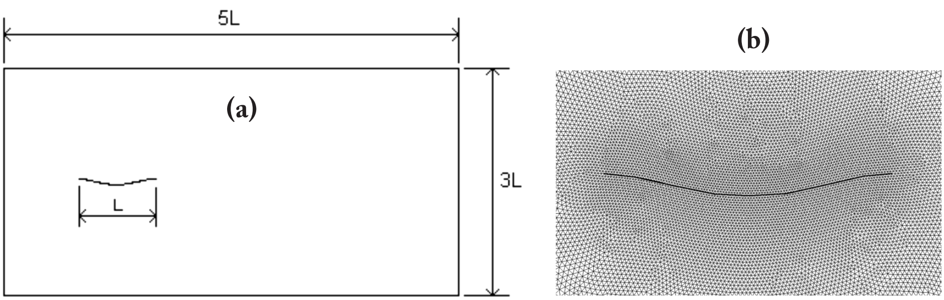

Figure 2. (a) Computational domain. (b) Detail of the grid around the fin.

The fluid flow was simulated using the commercial software Ansys Fluent 6.3. The numerical algorithm implemented in this code automatically updates the mesh after each time step in order to minimize convergence problems if a cell becomes too large, too small or excessively stretched.

Calculation Parameters

A first-order differencing scheme in time and second-order upwind differencing scheme in space was used and an implicit method was employed. Pressure velocity coupling of the continuity equation was achieved using the SIMPLE algorithm.

The period T was divided in 100 parts, *i.e.*, the time step was $\Delta t=T/100$. The grid size and the time step sensibility were studied and it was verified that both of them were adequate to obtain accurate enough results.

Boundary Conditions

Upstream the velocity components were fixed to be uniform, i.e., $u=U_\infty$ and $v=0$, while the gauge pressure was set to zero. Downstream, a zero gradient condition was taken for both velocity and pressure. On the fin surface, the no slip condition was used for the velocity components and finally, on the top and bottom surfaces the slip condition was imposed.

Calculation of the Hydrodynamic Forces

As the fin moves through the water, a force along the x and y directions is produced. The components of the force, F_x and F_y, can be evaluated by integrating the projection of the pressure and the shear stress in the x and y directions respectively. The total thrust component along the x direction was computed by adding the pressure and viscous forces contributions, Eq. (7):

$$F_x = F_{px} + F_{vx} \tag{7}$$

where F_p is the pressure force and F_v is the viscous force.

The pressure force along the x axis is given by:

$$F_{px} = -\int_A p n_x dA \tag{8}$$

where n_x is the x component of the unit normal vector on dA.

The viscous force along the x axis is given by:

$$F_{vx} = \int_A \tau_{xj} n_j dA \tag{9}$$

where τ_{xj} is the viscous stress tensor.

For the present non dimensional analysis, the force coefficients, defined by Eq. (10), were obtained.

$$C_F = \frac{F}{\rho U_\infty^2 L^2} \tag{10}$$

RESULTS AND DISCUSSION

In order to reach the steady state it has been necessary to consider a large time. It was verified that after approximately thirty wave periods the time is large enough to reach the steady state. For this reason, all the results given in the present paper correspond to the 30th period of time.

For almost all results presented in the present paper, the amplitude was taken as 0.02 m, the electrical motor frequency as 10 Hz, the free-stream velocity as 1 m/s and the fluid properties the corresponding ones to water at 25°C. For these conditions the Reynolds number is 52000, the Froude number is 0.44 and the non-dimensional frequency, defined by means of the Strouhal number, Eq. (11), is 1.2.

$$St = \frac{fA}{U_\infty} \tag{11}$$

Velocity field

The non dimensional velocity field for the instant 0.1t/T is shown in Fig. 3.

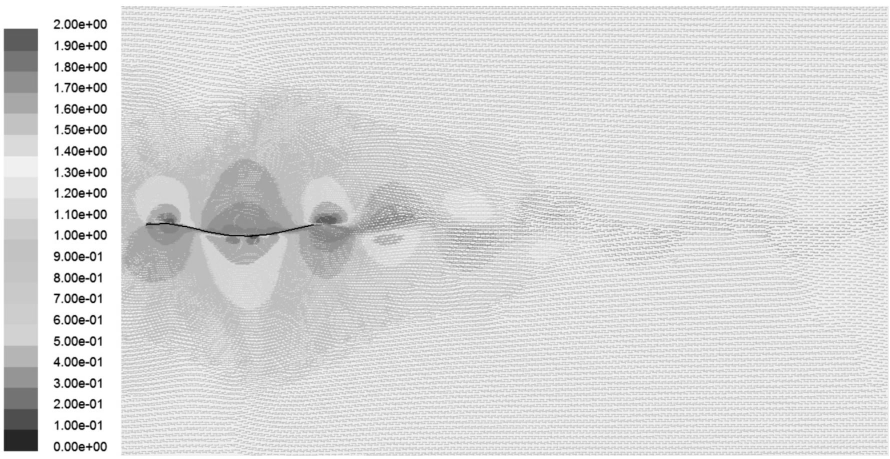

Figure 3. Velocity field for 0.1t/T, St = 1.2, Re = 52000 and Fr = 0.44.

From Fig. 4, it can be seen that a jet is formed at the right side of the fin. This jet is the source of the thrust because it creates a force which tends to move the fin from the right to the left. As the jet separates from the fin, its intensity decreases due to viscous dissipation.

Pressure field

Fig. 4 shows the non dimensional dynamic pressure field for the instant 0.1t/T, corresponding to Fig. 3. The effect of the undulating movement on the flow field can be clearly seen and confirms the of the velocity field tendency. The high and low pressure regions are greatly developed by the influence of the undulating fin motion and the free stream velocity.

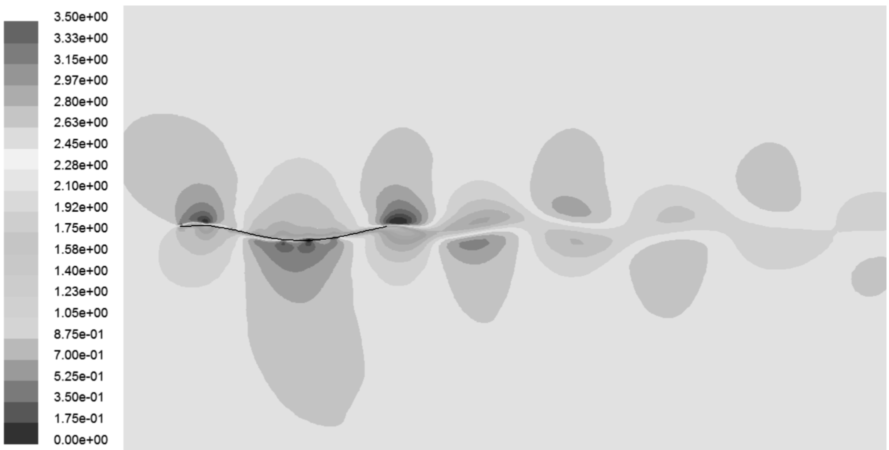

Figure 4. Dynamic pressure field for 0.1t/T, St = 1.2, Re = 52000 and Fr = 0.44.

From Fig. 4, it can be seen that the fin generates two spanwise vortices per oscillation which are arranged into a staggered array resembling a Karman vortex, but with the signs of the vorticity reversed. Some authors refer to this pattern as a reverse Karman vortex street (Triantafillou et al, 1993; Yong-hua Zhan, 2007).

Hydrodynamic forces

In order to systematically quantify the forces, Fig. 5 was created. This figure represents the time history of the instantaneous pressure force coefficient, the viscous force coefficient and the average total force coefficient.

The magnitude of the instantaneous force is dependent on the flapping frequency, flow velocity and amplitude, but in general it reaches its maximum value twice in each cycle because of the symmetrical undulating movement. The pressure force coefficient in Fig. 5 depicts two peaks of acceleration.

From Fig. 5, it can also be observed that the mechanism is accelerating for these conditions because the net thrust force is positive.

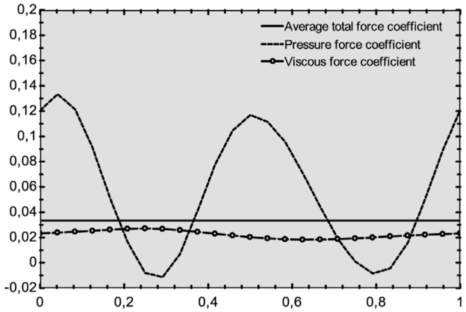

Figure 5. Time history of the pressure force, viscous force and average total force for St = 1.2, Re = 52000 and Fr = 0.44.

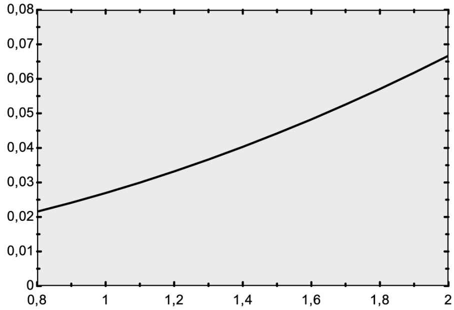

Figure 6. Variation of the total force coefficient with Strouhal number for Re=2000 and Fr=0.44.

The influence of the frequency on the force was studied. As expected, thrust increases when the frequency increases. This phenomenon is shown in Fig.6, which shows the total average force coefficient by means of the St number for values between 0.8 and 2, which corresponds to frequencies of 6.67 and 16.67 Hz respectively.

Experimental results

In order to compare the numerical results with experimental ones, the frequency was incremented from 6 to 15 Hz and numerical and experimental results were compared. Experimental results were based on the "fixed pull point" method, which consists on fixing the prototype to a bollard by means of a rope, Fig. 7, and measuring the force produced.

Numerically, this experiment was simulated imposing a zero free stream velocity. Numerical and experimental results of the average thrust force against the frequency are compared in Fig. 8.

Figure 7. Bollard pull trial under real conditions (fixed pull point).

From Fig. 8, it can be seen that thrust varies with the frequency following an exponential function. Numerical results are higher than experimental ones because first do not consider three-dimensional losses. In the experimental prototype it was observed that, apart from the longitudinal force, a small but not neglecting transversal force is produced. This force was zero for the numerical model because it was two-

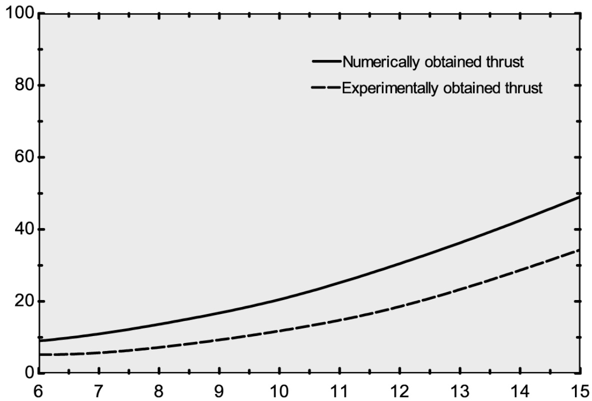

Figure 8. Variation of the average thrust with frequency for numerical and experimental results.

dimensional. Unfortunately, a three-dimensional model is quite computationally consuming and was not carried out in the present work.

CONCLUSIONS

This paper proposes an undulating marine propulsor based on the fin fish movement. The system consists of a flexible fin moved by an electric motor. It was implemented in a small ship built in our lab.

Although fish movement is very efficient because it has the advantage of optimization via natural selection, a CFD model was developed to improve fish movement and optimize the design of the mechanism. CFD was very useful to answer several important questions, for example the influence of the oscillation frequency, amplitude, wave length and other design parameters. For this reason, the propulsor is very efficient and maneuverable. Details of the velocity and pressure field provided by the CFD model were presented in the present paper. Pressure, viscous and total forces were presented too. Numerical results agreed well with experimentally obtained ones.

It was found that a more thorough study should be done in order to investigate tri-dimensional effects. Future works including turbulence modeling shall also be needed because it was found that the flow becomes turbulent for higher frequencies than the ones studied in the present paper. Adding turbulence and creating a three-dimensional simulation would provide a more accurate and realiscit numerical simulation. Nevertheless, the present work is an important step to study and design biologically-inspired mechanisms.

REFERENCES

Barret, D.S.; Triantafyllou, M.S.; Yue, D.K.P.; Grosenbaugh, M.A. and Wolfgang, M.J. (1999). Drag reduction in fish-like locomotion. *Journal of Fluid Mechanics* 392, 183-212.

Bordner, G.L. (1978). Non linear analysis of laminar boundary layer flow over a periodic wavy wall, *Physics of Fluids* 21, 1471.

Bozkurttas, M.; Tangorra, J.; Lauder, G. and Mittal, R. (2008). Understanding the hydrodynamics of swimming: from fish fins to flexible propulsors for autonomous underwater vehicles. *Advances in Science and Technology* 58, 193-202.

Caponi, E.A.; Fornberg, B.; Knight, D.D.; McLean, J.W.; Saffman, P.G. and Yuen, H.C. (1982). Calculations of laminar viscous flow over a moving wavy surface. *Journal of Fluid Mechanics* 124, 347-362.

Low, K.H. (2008). Locomotion simulation and system integration of robotic fish with modular undulating fin. *International Journal of Simulation* 7 (8), 64-77.

Markatos, N.C.G. (1978). Heat mass and momentum transfer across a wavy boundary. *Computer Methods in Applied Mechanics and Engineering* 14, 323-376.

McLean, J.W. (1983). Computations of turbulent flow over a moving wavy boundary. *Physics of Fluids* 26, 2065-2073.

Patel, V.C.; Chon, J.T. and Yoon, J.Y. (1991). Laminar flow over wavy walls. *Journal of Fluids Engineering* 113, 574.

Patel, V.C.; Chon, J.T. and Yoon, J.Y. (1991). Turbulent flow in a channel with a wavy wall. *Journal of Fluids Engineering* 113, 579.

Rodríguez, J.; González, P.; Couce, A.; González, G. (2009). Diseño de sistema de propulsión ondulante. *Proceedings of XIII International Congress on Project Engineering, June, Badajoz, Spain, pp. 1961-1972.*

Triantafyllou, M.; Triantafyllou, M.S.; Grosenbaugh, M.A. (1993). Optimal thrust development in oscillating foils with appliction to fish propulsion. *Journal of Fluid Struct.* 7, 205-224.

Yong-hua Zhang, Lai-bing Jia, Shi-wu Zhang, Jie Yang and Low, K.H. (2007). Computational research on modular undulating fin for biorobotic underwater propulsor. *Journal of Bionic Engineering* 4, 25-32.

Zhang, D.; Hu, D.; Shen, L.; Xie, H. (2007). Design of an artificial bionic neural network to control fish-robot's locomotion. *Neurocomputing,* 71, 648-654.

ASPECTOS DE DISEÑO Y SIMULACIÓN CFD BIDIMENSIONAL DE UN PROPULSOR MARINO BASADO EN UN MOVIMIENTO ONDULATORIO DE INSPIRACIÓN BIOLÓGICA

Resumen

Actualmente, es bien sabido que los animales acuáticos son más eficaces que los vehículos marinos. Existen un gran número de investigadores que han construido diferentes tipos de maquinas replicando el movimiento de los animales. El principal problema es que es muy importante entender completamente la hidrodinámica del movimiento si se quiere diseñar un mecanismo de manera óptima. Por este motivo, la dinámica de fluidos computacional (CFD) se ha convertido en una herramienta muy poderosa porque resuelve las ecuaciones gobernantes de conservación de la masa y cantidad de movimiento para obtener las características del flujo de fluido.

Este artículo presenta las características de un propulsor marino basado en una aleta ondulante que imita el movimiento de los peces. Además, se presenta una extensa investigación CFD del flujo de fluido alrededor del propulsor. Como las pruebas experimentales fueron hechas en un modelo a escala en lugar de un barco real, se hizo un análisis adimensional. Particularmente, los grupos adimensionales analizados fueron el número de Reynolds, el de Froude y el de Strouhal.

DEFINICIÓN DEL PROBLEMA

Diseño y cinemática

El grupo de investigación "Innovaciones Marinas" (Universidad de la Coruña – España) desarrolló un propulsor ondulante marino. Los aspectos fundamentales se muestran en la Fig. 1a, en la que aparece el prototipo, y la figura 1b, que muestra un detalle de la aleta ondulante de 0,52 m de longitud.

El movimiento ondulante es creado por medio de un sistema de bielas y cigüeñales que producen una forma de onda. Los detalles fueron presentados previamente (Rodríguez *et al.,* 2009). El movimiento es producido por un motor eléctrico y la frecuencia de oscilación es regulada por un controlador de frecuencia.

Una ventaja muy importante de este sistema es que es reversible, es decir, tiene la misma eficiencia operando marcha adelante o atrás. Esto lo hace ideal para vehículos que requieren alta maniobrabilidad.

Análisis CFD

El flujo alrededor de una pared ondulante es distinto al del flujo alrededor de una pared rígida. A medida que el fluido se mueve a lo largo de la superficie, se produce empuje debido a las ondulaciones desde la parte anterior a la parte posterior de la aleta. Para las mismas condiciones, un pez consume mucha menos energía para desplazarse que un cuerpo rígido debido a que el movimiento del pez reduce los efectos de turbulencia. Por este motivo, el diseño de la forma de la onda es muy importante. Se han realizado varios estudios CFD para varias configuraciones de onda antes de construir el prototipo experimental.

Ecuaciones gobernantes

El movimiento de flujo es gobernado por las ecuaciones de conservación de la masa y de Navier-Stokes, que para un fluido incomprensible, newtoniano y de propiedades constantes vienen dadas por las Ecs. (1) y (2) respectivamente.

$$\nabla \cdot \vec{V} = 0 \tag{1}$$

$$\frac{\delta \vec{V}}{\delta t} + \nabla \cdot (\vec{V}\vec{V}) = -\frac{\nabla p}{\rho} + \nu \nabla^2 \vec{V} + \vec{g} \tag{2}$$

Todas las variables fueron convertidas en adimensionales introduciendo los parámetros de referencia dados en la Tabla 1. Las variables adimensionales, denotadas con *, también se muestran en esta tabla.

Las ecuaciones gobernantes en forma adimensional resultan como sigue:

$$\nabla^* \cdot \vec{V}^* = 0 \tag{3}$$

$$\frac{\delta \vec{V}^*}{\delta t^*} + \nabla^* \cdot (\vec{V}^* \vec{V}^*) = -\nabla p^* + \frac{1}{\mathrm{Re}} \nabla^{*2} \vec{V}^* + \frac{1}{Fr^2} \vec{g}^* \tag{4}$$

donde Re es el número de Reynolds, definido por la Ec. (5). Representa la relación entre los efectos de inercia y los viscosos.

$$\mathrm{Re} = \frac{U_\infty L}{\nu} \tag{5}$$

Fr es el número de Froude, definido por la Ec. (6). Representa la relación entre efectos de inercia y de gravitatorios.

$$Fr = \frac{U_\infty}{\sqrt{Lg}} \tag{6}$$

IMPLEMENTACIÓN NUMÉRICA

Malla computacional

Para simular el movimiento de la aleta, fue necesario emplear una malla dinámica. El dominio computacional, que se muestra en la Fig. 2a, fue de 3L por 5L (siendo L la longitud de la aleta), y fue discretizado en 27000 nodos. Los elementos fueron triangulares y el tamaño de malla fue refinado en la zona cercana a la aleta. Un detalle de la malla en la zona cercana a la aleta se muestra en la Fig. 2b.

El software utilizado ha sido Ansys Fluent 6.3. El algoritmo numérico implementado en este software actualiza automáticamente la malla tras cada paso de tiempo con el fin de minimizar problemas de convergencia si una celda resulta demasiado grande, pequeña o deformada.

Parámetros de cálculo

Se ha utilizado un esquema de discretización de primer orden en tiempo y segundo reden en espacio, y se ha acudido a un método implícito. El acoplamiento entre presión y velocidad se ha tratado mediante el algoritmo SIMPLE.

El periodo T fue dividido en 100 partes, es decir, el paso de tiempo fue $\Delta t=T/100$. Tanto el tamaño de malla como el paso de tiempo fueron estudiados y se verificó que el tamaño de malla y de paso de tiempo empleados son insensibles ante refinamiento de los parámetros

Condiciones de contorno

Aguas arriba, las componentes de velocidad fueron fijadas como uniformes, es decir, $u=U_\infty$ and $v=0$, mientras que la presión manométrica se fijó como cero. Aguas abajo, se impuso una condición de gradiente nulo tanto para la presión como para la velocidad. En la superficie de la aleta, se impuso una condición de no deslizamiento y finalmente, en las superficies superior e inferior del dominio, se impuso la condición de deslizamiento libre.

Cálculo de las fuerzas hidrodinámicas

A medida que la aleta se mueve en el agua, se produce una fuerza en las direcciones x e y. Las componentes de la fuerza, F_x y F_y, fueron evaluadas integrando la proyección de la presión y de la tensión cortante en las direcciones x e y respectivamente. La componente de empuje a lo largo del eje x fue calculada sumando la contribución de la presión y de la viscosidad, Ec. (7):

$$F_x = F_{px} + F_{vx} \tag{7}$$

donde F_p es la fuerza de presión y F_v es la fuerza de viscosidad.

A su vez, la fuerza de presión a lo largo del eje x está dada por:

$$F_{px} = -\int_A p n_x dA \tag{8}$$

donde n_x es la componente x del vector unitario normal en dA.

La fuerza viscosa a lo largo del eje x viene dada por:

$$F_{vx} = \int_A \tau_{xj} n_j dA \tag{9}$$

donde τ_{xj} es el tensor de tensiones viscosas.

Para el presente análisis adimensional, se calcularon los coeficientes de fuerza, definidos por la Ec. (10).

$$C_F = \frac{F}{\rho U_\infty^2 L^2} \tag{10}$$

CONCLUSIONES

Este artículo propone un propulsor marino basado en el movimiento de las aletas de los peces. El sistema cosiste en una membrana flexible movida por un motor eléctrico. Fue implementada en un pequeño barco construido en un laboratorio.

A pesar de que el movimiento de los peces es muy eficaz porque es el resultado de la optimización de la selección natural, se ha desarrollado un modelo de CFD para mejorar el movimiento de los peces y así optimizar el diseño del mecanismo. El CFD ha sido de utilidad para contestar algunas preguntas importantes, como la influencia de la frecuencia de oscilación, amplitud, longitud de onda y otros parámetros de diseño. Por este motivo, el propulsor diseñado es muy eficiente. Los detalles del campo de presiones y de velocidades proporcionados por el modelo CFD se han mostrado en este artículo. Las fuerzas resultantes de presión, viscosidad también han sido presentadas. Los resultados obtenidos numéricamente mostraron buena concordancia con los obtenidos experimentalmente en el prototipo.

Se encontró que es necesario un estudio de la influencia de los efectos tri-dimensionales. Trabajos futuros incluyendo modelos de turbulencia también se ha visto que son necesarios porque para frecuencias mayores que las estudiadas el flujo se vuelve turbulento. Sin embargo, el presente trabajo es un importante paso para entender y diseñar mecanismos de inspiración biológica.